# Experimental study of a multiwavelength photon sieve designed by random-area-divided approach

**Article** *in* Applied Optics · April 2009

DOI: 10.1364/AO.48.001619 · Source: PubMed



**5 authors**, including:

Lifang Shi
institute of optics and electronics,Chinese ac…
**54** PUBLICATIONS **121** CITATIONS
SEE PROFILE

Chunlei Du
Chinese Academy of Sciences
**346** PUBLICATIONS **2,637** CITATIONS
SEE PROFILE

# Experimental study of a multiwavelength photon sieve designed by random-area-divided approach

Chongxi Zhou, Xiaochun Dong, Lifang Shi, Changtao Wang, and Chunlei Du*

State Key Lab of Optical Technologies for Microfabrication, Institute of Optics & Electronics, Chinese Academy of Sciences, Chengdu China, 610209

*Corresponding author: cldu@ioe.ac.cn

Received 5 December 2008; accepted 7 February 2009;
posted 17 February 2009 (Doc. ID 99083); published 9 March 2009

In this paper, a design method for a multiwavelength photon sieve is described based on a random-area-divided approach, where the whole aperture of a multiwavelength imaging photon sieve is divided into multiple discrete spaces corresponding to the number of the selected working wavelengths. The micropinhole distribution in each discrete space can be calculated for the defined wavelength with one fixed focal length in terms of the normal design for photon sieve. A three-wavelength photon sieve was designed and fabricated in the lab, and its imaging properties are analyzed in the experimental optical system with satisfactory results. 

*OCIS codes:* 050.1970, 220.4000, 350.3950, 110.4234.

## 1. Introduction

In this decade, diffractive optical elements (DOEs) have been promoted gradually with the fast development of microfabrication technologies and have become a main type of normal component in modern optical systems because of their unique characteristics of compact size, light weight, and high degree of design flexibility [1–6]. DOEs have also played an important role in the x-ray and EUV regions for many years [7–9]. To improve the resolution, in 2001, Kipp *et al.* proposed the novel idea of a photon sieve [10], where a zone plate originally composed of concentric rings is arranged properly by a great number of pinholes in a layer of metal film. Besides the advantage of resolving a spot smaller than the minimum feature size of the element, another great contribution of the idea is introducing a discrete concept for DOEs. According to the fundamental concept, recent work on structured lenses [11,12] by using subwavelength square-shaped holes in the metallic film has been reported. We believe that discrete structures can bring quite large freedom for realizing smooth space filtering and optimizing chromatic aberration to some degree. For exploiting the properties of the special type of DOE, in this paper, we demonstrate experimentally a multiwavelength photon sieve by designing the pinhole distribution in a certain area for the given wavelengths in order to obtain diffractive chromatic aberration that would be difficult to realize with a traditional zone plate.

## 2. Principle

### A. Basic Description of a Common Photon Sieve

According to the basic model of the photon sieve that was proposed by Kipp *et al.* [10], the microholes are located at the center of the rings given by the radial distance $r_n$, which is a distance from the center of the element to center of the $n$th ring of the zone plate, and their diameters are allowed to be larger than the corresponding ring width $w$ of the zone plate:

$$r_n{}^2 = 2nf\lambda + n^2\lambda^2. \quad (1)$$

The field value of the $n$th microhole at the focal plane is $U_n(0,0)$:

0003-6935/09/081619-05$15.00/0

$$U_n(0,0) \propto \frac{d}{w} J_1\left(\frac{\pi}{2}\frac{d}{w}\right), \tag{2}$$

where $J_1$ is the first-order Bessel function, $d$ is the diameter of the pinhole, $f$ is the focal length of the zone plate, and $\lambda$ is the working wavelength. Incident light passing through the microholes plays a positive role for $U_n(0,0) > 0$ and a negative role for $U_n(0,0) < 0$. As is known from Eq. (1), $U_n(0,0)$ has maximum value at $d/w \approx 1.5, 3.5, 5.5, 7.5\ldots$, and the final spatial resolution, which depends on the ratio of $d/w$, can be smaller than the smallest microhole diameter $d_{\min}$ according to Ref. [10]. Based on the detailed deduction in Refs. [13,14], the phase conditions for each pinhole being satisfied are given by the following formulas:

$$k\left(Ln + \frac{{r_n}^2}{2q}\right) = 2m\pi, \qquad Jinc\left(\frac{ka_n}{q}R_n\right) > 0, \tag{3}$$

$$k\left(Ln + \frac{{r_n}^2}{2q}\right) = \left(2m+1\right)\pi, \qquad Jinc\left(\frac{ka_n}{q}R_n\right) < 0, \tag{4}$$

where $a_n = d/2$ is the radius of the $n$th pinhole; $k = 2\pi/\lambda$ is the wavenumber; and $L_n, R_n, q$ are the quantities related to the spatial positions. With the above analysis, a common photon sieve can be designed based on the required imaging parameters: focal length $f$, aperture $D$ of the whole element, and the incident wavelength $\lambda$.

Generally, for a diffractive optical lens, the given focal length of $f$ can be valid only for the designed wavelength $\lambda$, thus the incident light with wavelengths of $\lambda + \delta\lambda$ will focus on the different positions of $f + \delta f$ and create stray light in the original focal plane as a background noise. The deviation $\delta f$ between the different focal lengths can be expressed simply by

$$\delta f = \frac{df}{d\lambda}\delta l = -\frac{f}{\lambda}\delta\lambda. \tag{5}$$

For the common photon sieve, it will also follow the properties of a diffractive lens and can be used only in a narrow band.

### B. Random-Area-Divided Approach

Since a photon sieve formed with a series of discrete structure offers more variants in the diameters and the positions of the microscale pinholes in the polar coordinate system, it has more freedom to be modulated in a different manner compared to the conventional zone plates. In order to form an image with multiple wavelengths by using one photon sieve, we employ the discrete property of the photon sieve. The basic idea for the random-area-divided method are described as follows: first, the whole aperture is divided into numbers of discrete parts as shown in Fig. 1, and the value of the number $M$ depends on the dividing angle interval $\Delta\theta$ in the direction of circumference and the dividing distant interval $\Delta R$ in the radial direction. The total dividing subareas can be described by the expression

$$M = 360^{\circ}/\Delta\theta * R/\Delta R. \tag{6}$$

Here $R$ is the radius of the considered lens. If $N$ is defined as the number of the incident wavelengths to be imaged, a number $Q$ can be determined by $M/N$, which corresponds to the space in the aperture used for different wavelengths. The design procedure is the following: first, $N \times Q$ pieces of discrete parts for $N$ types of wavelengths are selected randomly in the whole aperture, then each lens for different wavelengths from 1 to $N$ in the formal photon sieve with the same given focal length can be calculated based on the Kipp *et al.* formulas given in Subsection 2.A. After the design, the number $N$ of photon sieve lenses can be obtained, and a combination lens can be formed by adding these data together. In the design process, there are two important factors should be emphasized: first, the pinhole's position corresponding to the given wavelength should be selected in its own private space so that the special discrete parts for different wavelengths are not overlapped; Second, the total transmission area of the microholes on the different discrete parts should be equal to ensure that the color of the images is balanced in energy.

### C. Design Example for the Photon Sieve with Three Wavelengths

A multiwavelength photon sieve for three wavelengths with diameter 20 mm, focal length 200 mm and three wavelengths of red light ($\lambda_3 = 0.633\,\mu$m), green light ($\lambda_1 = 0.532\,\mu$m), and blue light ($\lambda_2 = 0.488\,\mu$m) is designed for use in the visible light band, and the results are given in Fig. 2, where Fig. 2(a)

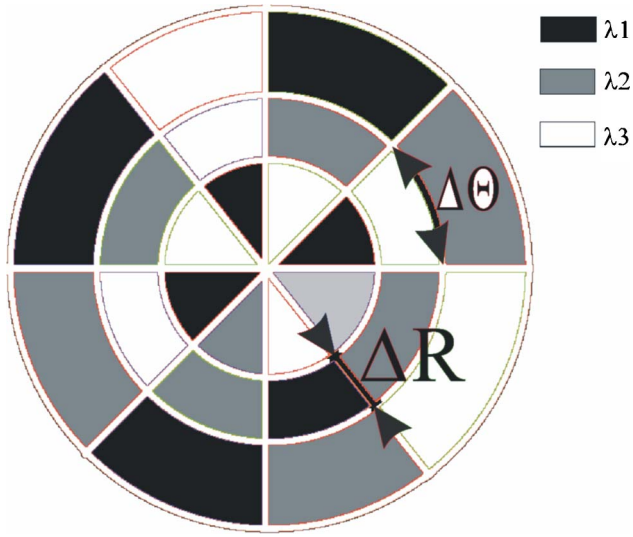


Fig. 1. (Color online) Description of a multiwavelength photon sieve using the random-area-divided approach.

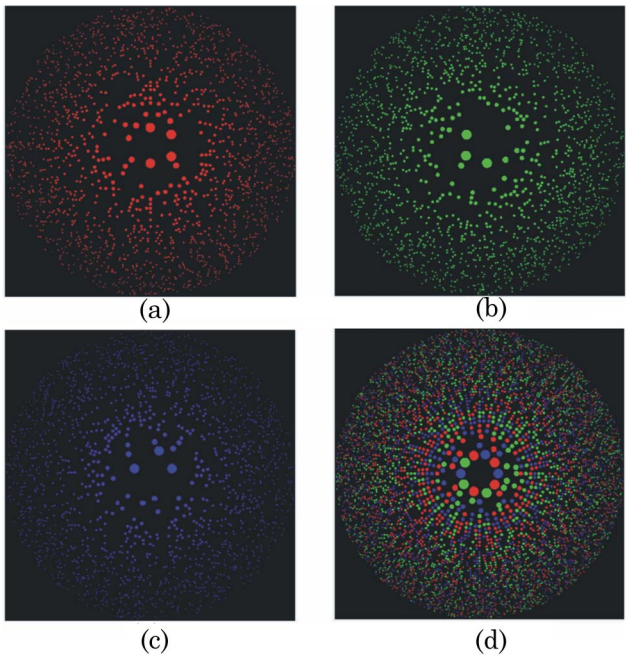


Fig. 2. (Color online) Design results of the multiple wavelength photon sieves for three wavelengths: (a) pinhole distribution of the first discrete part of the photon sieve for $\lambda_1$, (b) pinhole distribution of the second discrete part of the photon sieve for $\lambda_2$, (c) pinhole distribution of the third discrete part of the photon sieve for $\lambda_3$, and (d) combined pinhole distribution of the one sieve for three wavelengths.

shows the first part of the photon sieve for imaging to the light of $\lambda_1$, Fig. 2(b) shows the second part of the photon sieve for imaging to the light of $\lambda_2$, and Fig. 2(c) is the third part of the photon sieve for imaging to the light $\lambda_3$; Fig. 2(d) is a combination of the whole aperture of the multiwavelength photon sieve for the three imaging wavelengths. The calculations for the central positions and the radii of the corresponding pinholes were made based on Eqs. (3) and (4).

In order to acquire the proper resolution, pinhole diameters of $3.5w$ are adopted, where $w$ is the ring width of the zone plate. The different wavelengths result in different focal positions, and the focal length deviation among the three wavelengths is obtained from Eq. (5). With the microhole structures designed for the green light in the photon sieve, the incident green light will be focused on the ideal focal plane $f = 200$ mm, but the red and blue light will be focused on the front and rear positions away from $f$, respectively, as shown in Fig. 3(a). In this situation, three focal spots will appear along the optical axis for each color light. Thus when incident light corresponding to different wavelengths hits the whole aperture of the three-wavelength photon sieve, nine focal spots will be created, of which the three focal spots formed by the lights will fall on the ideal focal position. Figure 3(a) is the intensity distribution along the optical axis of the three wavelengths lights from the whole aperture of the three-wavelength photon sieve, and Fig. 3(b) is the intensity distribution on the focal plane of the three light wavelengths. The focal intensities formed by the three different wavelengths of light decrease to 1/3 of the single-wavelength photon sieve, but the total intensity is equal to that of the single-photon wavelength sieve. The spot sizes (FWHM) are 9 $\mu$m, 7 $\mu$m, and 6 $\mu$m for red, blue, and green light, respectively, which are close to the diffractive limits.

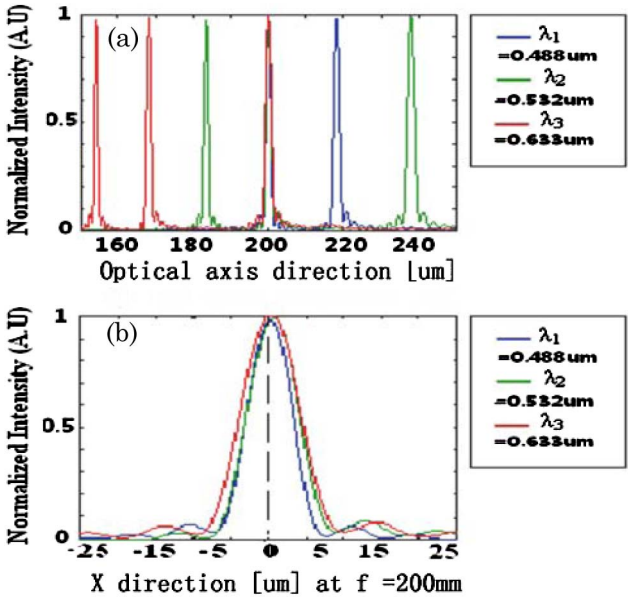


Fig. 3. (Color online) Intensity distributions of the MWPS and the chromatic characteristics. (a) Intensity distribution of MWPS on the optical axis of three wavelengths of light illumination. (b) Intensity distribution of MWPS on the focal plane with three wavelengths of light as light sources.

## 3. Experiment Description

### A. Fabrication for the Multiwavelength Photon Sieve

In order to fabricate the multiwavelength photon sieve, the designed data were transferred to the Common Intermediate Format of the laser direct writing system first. A quartz glass substrate with a layer of 100 nm chromium was prepared. By means of laser direct writing photolithography, the pinholes' distribution pattern on the photon sieve could be formed on the resist of the substrate. And after the development and etching processing, the multiwavelength photon sieve element was manufactured as shown in Fig. 4. The enlarged part is a magnified image taken by microscopy.

### B. Imaging Experiment with the Multiwavelength Photon Sieve

For evaluating the function of the multiwavelength photon sieve considered, an experimental setup is built as shown in Fig. 5. The incident laser beam is first focused by a microscopy objective and then passes through a pinhole filter before it is collimated with a collimation lens. The expanded laser beam illuminates a resolution test target as an object formed by grating groups with different size. In order to

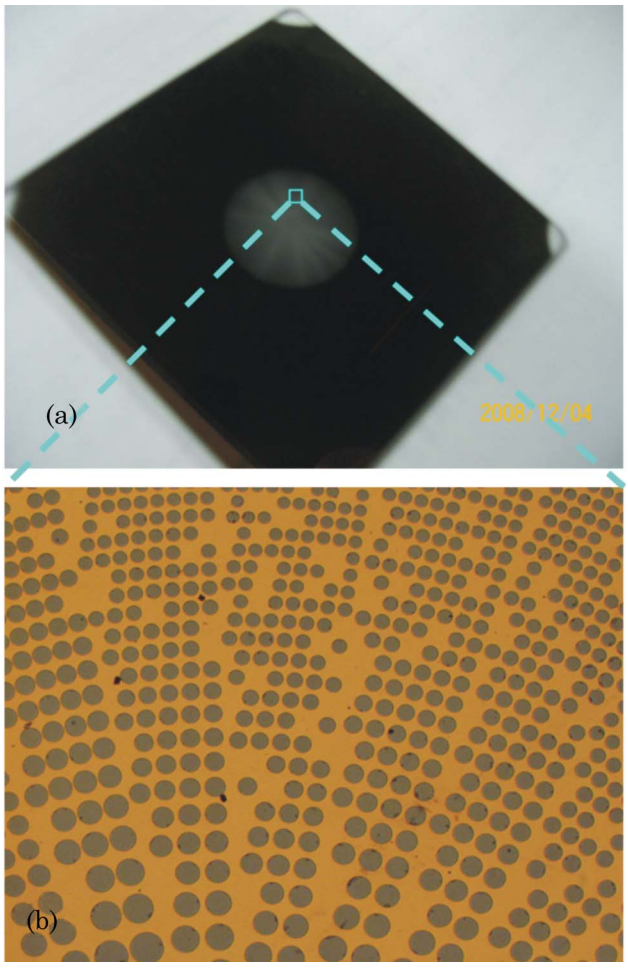


Fig. 4. (Color online) Photo of the fabricated multiwavelength photon sieve and its magnified image.

eliminate the zero-order diffractive light, the object is put off axial with a magnification of 1 : 1. A diffuser is used to eliminate the speckle caused by laser coherence. In order to investigate the imaging characteristics for different wavelength, A He–Ne laser, a Nd: YAG frequency doubling laser, and an $Ar^+$ laser have been used as three illumination sources with wavelengths of 0.633 $\mu$m, 0.532 $\mu$m, and 0.488 $\mu$m, respectively. The incident laser beam diffracted by the object arrives the multiwavelength photon sieve with a diameter of 20 mm and a focal length of 200 mm, and the first-order diffractive images formed by the

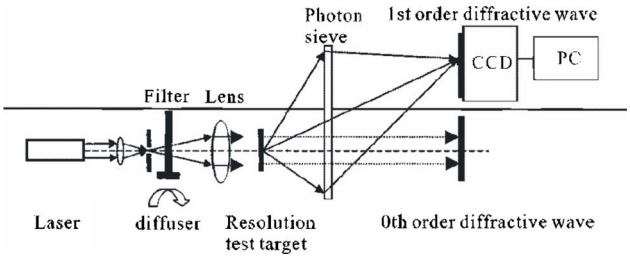


Fig. 5. (Color online) Experimental setup of the multiwavelength photon sieve imaging system.

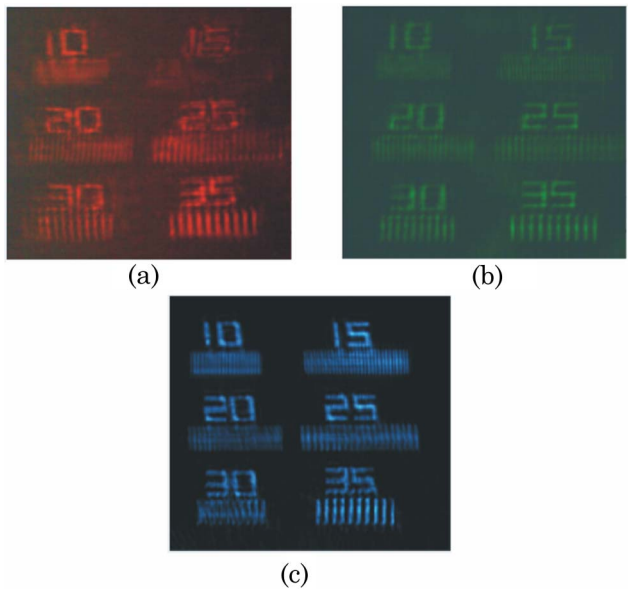


Fig. 6. (Color online) 1 : 1 scaled images of the resolution plate imaged by the photon sieve: (a) red light illumination, (b) green light illumination, (c) blue light illumination.

multiwavelength photon sieve can be detected at the imaging plane by a color complementary metal oxide semiconductor camera with pixel size 3.5 $\mu$m× 3.5 $\mu$m. In Figs. 6(a)–6(c), the imaging results taken by using the multiwavelength photon sieve are given corresponding to different incident laser beams with wavelengths of 0.633 $\mu$m, 0.532 $\mu$m, and 0.488 $\mu$m, respectively, where the dimensions of the numerals in the figure are in micrometers. It is obvious that a resolution of 10 $\mu$m can be recognized with the multiwavelength photon sieve, and the imaging quality achieved by using the blue laser is better relative to the imaging quality achieved by using the red and green lasers, which agrees with the rule of resolution criterion.

## 4. Conclusion

We have demonstrated that a multiwavelength photon sieve based on the random-area-divided optimization design can be used to realize an imaging with multiple narrowband wavelengths. It turns out that the photon sieve in the discrete formation can be modulated with a greater degree of freedom to break the limit of single-wavelength imaging that the traditional DOEs suffered. Although the proposed random-area-divided approach is not a perfect tool to manipulate chromatic aberration to an ideal degree with satisfactory energy efficiency, the experience obtained through our operation will reveal a good foreground by using the discrete structures as a lens or other phase modulation elements. In our experiment, the photon sieve lens can keep its original properties of smaller sidelobes and higher imaging contrast with the resolution close to the diffractive limit. Probably the arrangement of the multiwavelength photon sieve will provide an alternative

way for imaging with the illumination sources of a few separate wavelengths, for example, color laser displays and color laser printing.

This work was supported by the 863 Program of China (2007AA03Z332) and Chinese Nature Science Grants 60678035 and 60727006. Authors would like to thank Yixiao Zhang of Sichuan University for her kind contribution for the experimental work.

## References

1. R. Silvennoinen, V. Vetter, S. Heikki, H. Tuononen, M. Silvennoinen, K. Myller, L. Cvrcek, J. Vanek, and P. Prachar, "Sensing of human plasma fibrinogen on polished, chemically etched and carbon treated titanium surfaces by diffractive optical element based sensor," Opt. Express **16**, 10130–10140 (2008).
2. A. J. Caley and M. R. Taghizadeh, "Diffractive optical elements for simultaneous operation in reflection and transmission," Appl. Opt. **47**, 1553–1558 (2008).
3. J. S. Liu, A. J. Caley, M. R. Taghizadeh, E. Gu, J. M. Girkin, and M. D. Dawson, "Design of diffractive optical elements for beam shaping of micro-pixellated LED light to a tightly focused spot," J. Phys. D: Appl. Phys. **41**, 094005 (2008).
4. T. G. Jabbour, "Axial field shaping under high-numerical-aperture focusing," Opt. Lett. **32**, 527–529 (2007).
5. L. Shi, C. Du, X. Dong, Q. Deng, and X. Luo, "Effective formation method for an aspherical microlens array based on an aperiodic moving mask during exposure," Appl. Opt. **46**, 8346–8350 (2007).
6. H. T. Gao, X. C. Dong, Y. D. Zhang, Q. L. Deng, L. Pan, X. D. Lin, and C. L. Du, "A turbulence simulation plate based on irregular micro optical structures fabricated by mask moving technique," Opt. Eng. **47**, 016004 (2008).
7. G. Schmahl, D. Rudolph, P. Guttmann, and O. Christ, "Zone plates for x-ray microscopy," in *X-Ray Microscopy*, Vol. 43 of Springer Series in Optical Sciences, G. Schmahl and D. Rudolph, eds. (Springer-Verlag, 1984), pp. 63–74.
8. E. H. Anderson, V. Boegli, and L. P. Muray, "Electron beam lithography digital pattern generator and electronics for generalized curvilinear structures," J. Vac. Sci. Technol. B **13**, 2529–2534 (1995).
9. E. H. Anderson, D. L. Olynick, B. Harteneck, E. Veklerov, G. Denbeaux, W. Chao, A. Lucero, L. Johnson, and D. Attwood, "Nanofabrication and diffractive optics for high resolution x-ray applications," J. Vac. Sci. Technol. B **18**, 2970–2975 (2000).
10. L. Kipp, M. Skibowski, R. L. Johnson, R. Berndt, R. Adelung, S. Harm, and R. Seemann, "Sharper images by focusing soft X-rays with photon sieves," Nature **414**, 184–188 (2001).
11. Y. Chen, C. Zhou, X. Luo, and C. Du, "Structured lens formed by a 2D square hole array in a metallic film," Opt. Lett. **33**, 753–755 (2008).
12. S. Yin, C. Zhou, X. Luo, and C. Du, "Imaging by a sub-wavelength metallic lens with large field of view," Opt. Express**16**, 2578–2583 (2008).
13. Q. Cao and J. Jahns, "Nonparaxial model for the focusing of high-numerical-aperture photon sieves," J. Opt. Soc. Am. A **20**, 1005–1012 (2003).
14. Q. Cao and J. Jahns, "Focusing analysis of the pinhole photon sieve:individual far-field model," J. Opt. Soc. Am. A **19**, 2387–2393 (2002).